

Transactions, SMiRT-26
Berlin/Potsdam, Germany, July 10-15, 2022
Division V

FRAGILITY ANALYSIS OF NSSS

Manuel Pellissetti¹, Bojan Radmanovic², Andrii Nykyforchyn³, Sunay Staeuble-Akca⁴

¹ Senior Expert Seismic Safety, Framatome GmbH, Erlangen, Germany

² Senior Structural Engineer, Framatome GmbH, Karlstein, Germany

³ Director of Deterministic Safety Analyses, Gösgen-Däniken Nuclear Power Plant, Switzerland

⁴ Senior Earthquake Engineer, Gösgen-Däniken Nuclear Power Plant, Switzerland

ABSTRACT

Fragilities are a major ingredient of the seismic safety re-evaluation for the updated seismic hazard (“ENSI-2015”) in Switzerland.

The present paper deals with the fragility analysis of the nuclear steam supply system (NSSS) at Gösgen nuclear power plant (KKG), a three-loop pressurized water reactor (PWR). The analysis covers the stability and integrity of the main NSSS components and piping: reactor pressure vessel (RPV), steam generators (SG), reactor coolant pumps (RCP), pressurizer, main coolant lines, surge line, main feedwater and main steam lines (inside the reactor building). Furthermore, the fragility of the reactor trip is analyzed with respect to failure modes associated with the RPV internals (RPVI).

The fragilities are based on a probabilistic soil-structure interaction analysis with a coupled model of the reactor building and the above mentioned NSSS components / piping, see Rangelow et.al. (2019). The ground motion is represented by time histories corresponding to the median uniform hazard spectra (UHS) with an annual probability of exceedance of 10^{-4} .

The fragility analysis is performed according to the separation-of-variables method, following guidance documents such as EPRI (2009).

For the RPV internals, the fragility is based on two non-linear analysis models: a refined one for the evaluation of the fuel assembly (FA) spacer grids and a more global one for the remaining failure modes. A combined fragility has also been derived for the RPV internals, as the union of the individual failure modes.

The paper discusses the method, the input data and selected results of the analysis.

INTRODUCTION

Following an extensive Probabilistic Seismic Hazard Analysis (PSHA) conducted for the Swiss NPP sites, in 2016 the Swiss nuclear regulator ENSI has approved the updated seismic hazard estimates, under the label “ENSI-2015”. Together with the approval of the ENSI-2015 hazard definition, the Swiss regulator issued a request for the re-assessment of the seismic safety, subdivided in two analysis tasks:

1. A **deterministic** safety analysis to prove the safe shutdown of the nuclear power plant and the compliance with regulatory radiological limits for different review level earthquakes. This demonstration requires major efforts, given that the seismic ground motion for ENSI-2015 is far higher than the one considered in the seismic design.
2. An update of the seismic PSA (**Probabilistic** Safety Analysis) for re-evaluation of the contribution of seismic initiating events to plant operational risk.

A key ingredient of the 2nd task is the up-to-date fragility analysis of selected systems, structures and components. The components of the nuclear steam supply system (NSSS) are generally considered to have a high seismic capacity. On the other hand, the consequences of a seismic-induced failure of a major NSSS component are potentially so severe that the successful mitigation of such an accident sequence is questionable. In other words, in the PSA model such an event is typically assumed to lead directly to a core damage. Therefore it is important to quantify as much seismic margin as possible, so as to keep the risk footprint of NSSS failures low.

An extensive re-evaluation of the seismic design of the NSSS has been conducted as part of the deterministic safety analysis, see Fuetterer et.al. (2019). The re-evaluation included on one hand the deterministic re-analysis of the seismic loads (section forces) at the component supports, for the updated seismic hazard ENSI-2015. On the other hand, the complete set of original seismic design calculations was reviewed and the fulfillment of the design criteria was verified for the relevant elements of the load-transfer, in view of the increased loads due to ENSI-2015.

On the basis of such a comprehensive deterministic re-evaluation, a full-scope fragility analysis of the NSSS components could be performed with reasonable additional effort. The main **additional** effort consisted in the development of probabilistic in-structure responses and section forces at the NSSS supports. With these data the above mentioned verification of the seismic design calculations could be extended to the probabilistic loads, notably the 50% and 84% fractiles. The corresponding margins with respect to the design criteria were then used in the fragility analysis by separation-of-variables, as described in the following section.

FRAGILITY ANALYSIS METHODOLOGY

The standard fragility model used in the nuclear industry is the one presented by Kennedy and Ravindra (1984). It is based on the following expression for the seismic capacity:

$$A = \check{A} \varepsilon_R \varepsilon_U \quad (1)$$

where \check{A} is the median capacity, while ε_R and ε_U are log-normally distributed random variables with unit median and logarithmic standard deviations of β_R and β_U , respectively. ε_R and ε_U model the variability due to randomness and due to uncertainty, respectively. Typically, the capacity is defined in terms of the horizontal peak ground acceleration (PGA), more specifically of one horizontal component. The above model leads to the following expression for the conditional failure probability (“fragility”), in case of a seismic event leading to a PGA equal to a ,

$$F(a) = \Phi \left(\frac{\ln\left(\frac{a}{\bar{A}}\right) + \beta_U \Phi^{-1}(Q)}{\beta_R} \right) \quad (2)$$

where Φ is the cumulative distribution function of the standard normal distribution and Q is the confidence level. The above expression $F(a)$ is the basis for evaluating the so-called HCLPF capacity (“High Confidence of Low Probability of Failure”). It is defined as the value of the PGA for which there is a high confidence (95%) that the probability of failure does not exceed 5%. In simple terms, the HCLPF capacity is a conservative estimate for the seismic capacity of a component or structure. By inversion of Equation (2) the following expression for the HCLPF capacity is obtained:

$$a_{HCLPF} = \bar{A} \exp(-1.645 \cdot (\beta_R + \beta_U)) \quad (3)$$

The standard method for estimating the fragility parameters is the separation-of-variables method, described by Kennedy and Ravindra (1984) and EPRI (2009). It is based on expressing the capacity as

$$A = A_{REF} \cdot F \quad (4)$$

The scaling factor F is the maximum scalar, by which the reference ground motion – represented by A_{REF} – can be multiplied without producing failure. F is decomposed into response factors, F_{RS} (structure response) and F_{RE} (equipment response), and the capacity factor F_C .

$$F = F_{RS} \cdot F_{RE} \cdot F_C \quad (5)$$

The capacity factor F_C is further decomposed

$$F_C = F_S \cdot F_\mu = \frac{S - P_N}{P_T - P_N} \cdot F_\mu \quad (6)$$

where S is the strength of the structural element for the specific failure mode, P_N is the normal operating load (i.e., dead load, operating temperature load, etc.) and P_T is the total load on the structure (i.e., sum of the seismic load and the normal operating load).

In the present analysis the median strength factor is evaluated using the loads corresponding to the median responses corresponding to A_{REF} . Therefore, the medians of F_{RS} and F_{RE} are unity. The variability of F_{RS} is entirely represented by the variability of the probabilistic in-structure responses, as described below. The variability of F_{RE} is based on generic estimates given in guidance literature, such as EPRI (2009). The same applies to the variability of F_S and to the parameters (median and variability) of F_μ .

SEISMIC RESPONSE ANALYSIS

Ground motion (reference earthquake)

The reference earthquake (denoted as A_{REF} in the previous section) is based on the **median** UHS (uniform hazard spectra) at an AEP (annual exceedance probability) of 10^{-4} / year, see Figure 1 below. The underlying UHS are the result of the PSHA mentioned in the introduction, see NAGRA (2004) and Swissnuclear (2014). See also Stäubli-Akcaç et.al. (2019).

More specifically, **30 statistically independent sets** of time histories (TH) are used. The TH are based on recorded motions from the strong motion database RESORCE and are spectrally matched to the

median UHS at 10^{-4} / year. Each of the 30 TH is combined with one sample of soil parameters (shear modulus and soil damping) and structural parameters (Young's modulus and structure damping), generated with Latin Hypercube Sampling (LHS). The correlation between shear modulus and soil damping is taken into account; the same applies to Young's modulus and structure damping.

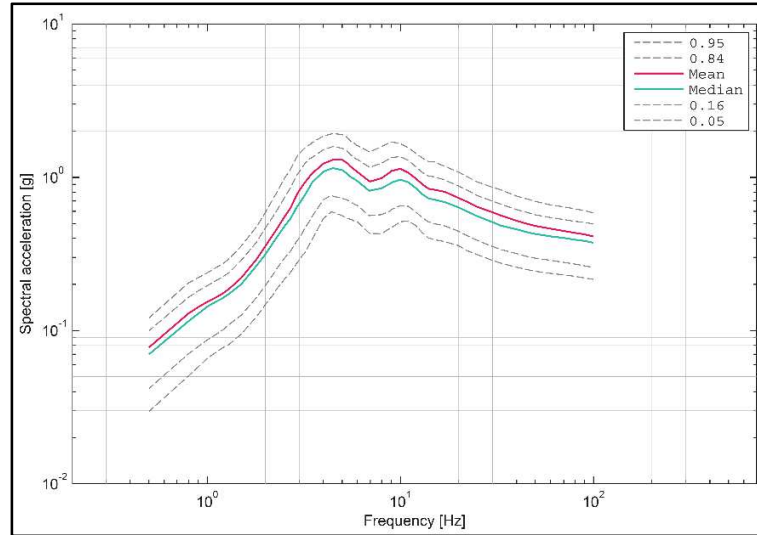


Figure 1. UHS for an AEP of $10^{-4}/a$ at the ground surface, Horizontal, $D = 5\%$.

Coupled model for main NSSS components

For the seismic re-evaluation the Swiss regulator requires a coupled seismic analyses of the NSSS and the reactor building, accounting for SSI (soil-structure interaction). The coupled model is described in detail in Rangelow et.al. (2019) and Fuetterer et.al. (2019). The NSSS model includes the main NSSS components and piping: reactor pressure vessel (RPV), steam generators (SG), reactor coolant pumps (RCP), pressurizer, main coolant lines, surge line, main feedwater and main steam lines (inside the reactor building).

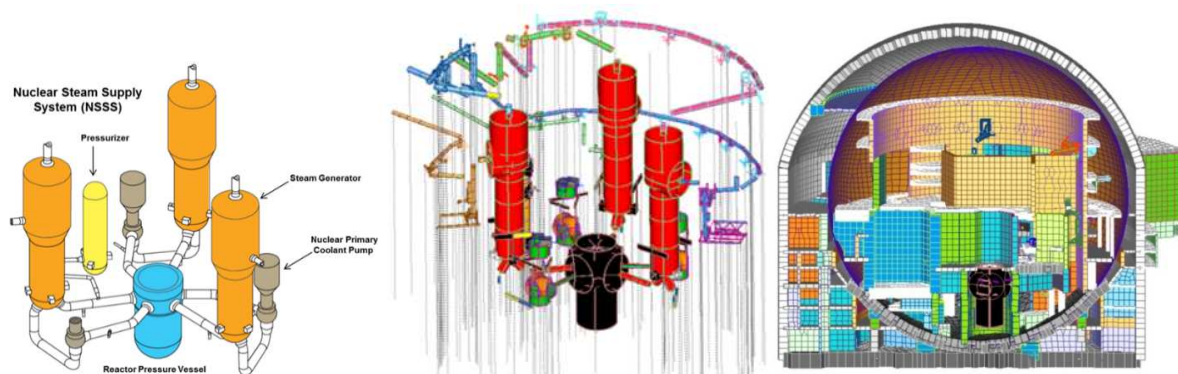


Figure 2. Schematic view of NSSS (left); NSSS model (center); coupled model of reactor building and NSSS (section view, NSSS partially hidden)

Probabilistic in-structure responses and section forces

The coupled model described in the previous section is used to produce probabilistic in-structure responses at numerous locations in the reactor building, including the supports of the NSSS. Furthermore, the time-dependent section forces at the elements modeling the supports are obtained.

The following Figure 3 shows the acceleration response spectra at the support of the RPV, for the set of 30 probabilistic time history analyses, see also Schmidl et. al. (2022).

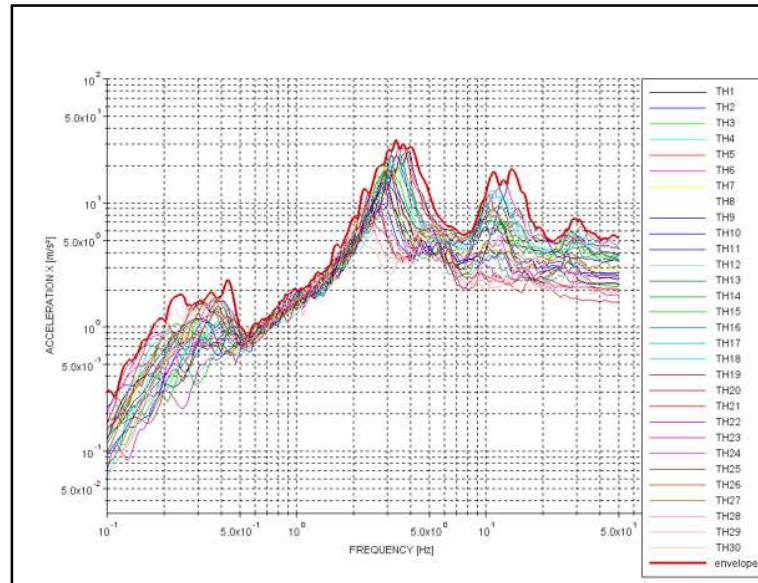


Figure 3. Probabilistic acceleration response spectra at RPV support, D=4%, horizontal component

As described in more detail in Fuetterer et.al. (2019), LOCA (loss-of-coolant-accident) loads on the NSSS components are generally significantly more severe than the seismic loads due to the reference earthquake. In most cases this implies ample seismic margins, independently from the stress utilization (ratio of total stress under seismic conditions, recall Equation (6), over the allowable stress) determined in the stress analysis.

Refined models for RPV internals and fuel assemblies

The evaluation of seismic-induced loads on the RPV internals and on the fuel assemblies is conducted downstream of the analyses with the coupled building-NSSS model. The in-structure response at the RPV support is used as input loading for time-history analyses with a refined model of the RPV internals. Material nonlinearities, sliding, friction and gap/impact effects are taken into account. Details on the model are given in Schmidl et.al. (2022).

The evaluation of the loads on the fuel assemblies is performed with yet another model, downstream of the RPV internals analysis. Details on that model are given in Pellissetti et.al. (2021). The main purpose of the model is to capture the seismic loading experienced by fuel assemblies in the form of impacts, either with neighboring fuel assemblies or – in case of fuel assemblies along the edge of the core – with the core barrel.

The impacting parts are the so-called spacer grids positioned along the fuel assemblies. As a consequence, the seismic robustness of the fuel assemblies is governed by spacer grid buckling. Resulting permanent spacer grid deformations at control-rod positions could slow down or hinder the control rod insertion. Therefore, the safety demonstration consists in limiting the permanent spacer grid deformations to levels for which a disturbance of the rod insertion is excluded.

RESULTS AND DISCUSSION OF INDIVIDUAL FAILURE MODES

For a number of failure modes, a fragility analysis has been performed with the methodology and input data described in the previous section.

The following Figures 4 and 5 shows the **normalized** HCLPF (high confidence of low probability of failure) values and the variability parameters β_R (aleatory) and β_U (epistemic).

The HCLPF capacities are normalized with respect to the **lowest** HCLPF capacity of all the failure modes considered in the fragility analysis, i.e. the RPV internals (failure mode “strength”).

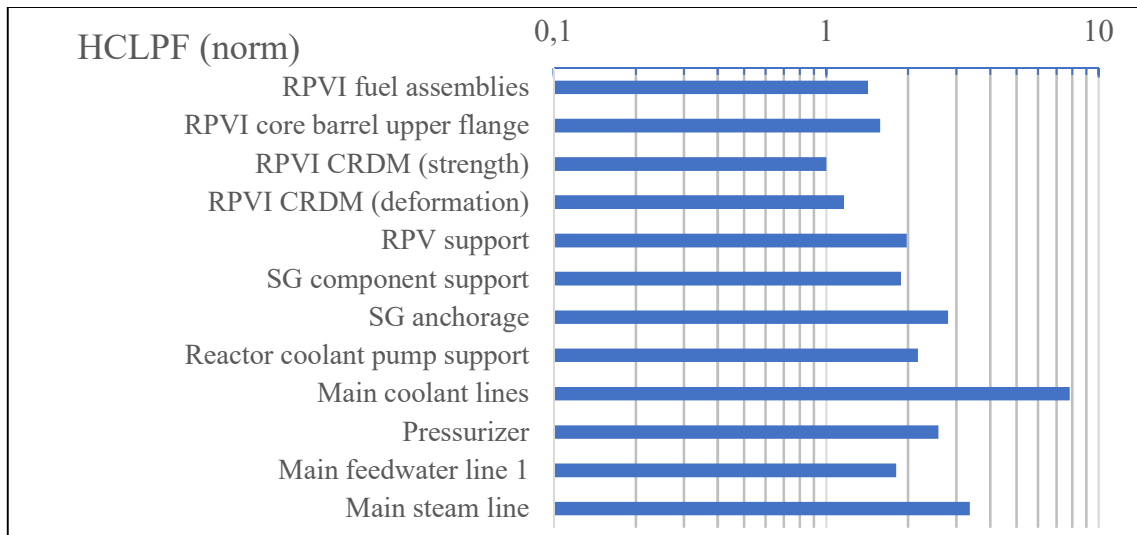


Figure 4. HCLPF capacities (normalized with respect to the lowest one).

The variability parameters are shown in the form of a **stacked** bar chart in the following Figure 5.

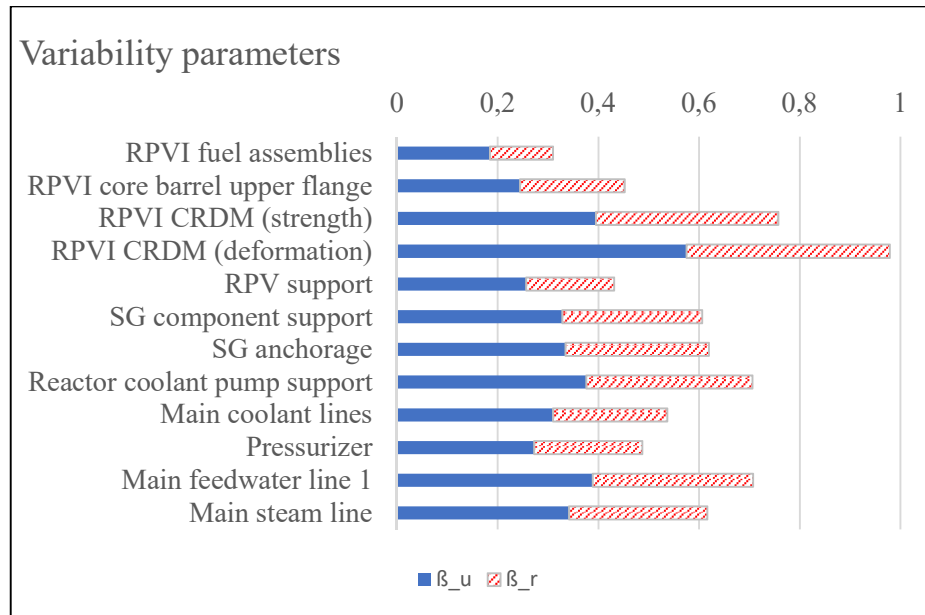


Figure 5. Variability parameters.

Overall observations

The HCLPF capacities of the RPVI are lower than those of the supports of the large NSSS components and of the NSSS piping. This is related to the previously mentioned fact that the seismic loads on the NSSS supports are abundantly enveloped by the conservative original design basis being a superposition of the original seismic design loads with the loads due to postulated large-break LOCA.

The high capacities of NSSS and main secondary **piping** (inside the reactor building) confirm the general consensus that piping – and in particular class 1 piping – has large seismic margins.

Regarding the variability parameters, a general observation is that the range of values is very large. This is remarkable, since there is no indication that the **input** variability – i.e. the variability of the in-structure responses (Figure 3) – is significantly different at the various support locations. On the other hand, it is recalled that there is a pronounced **frequency dependence** of the variability of in-structure response spectra, see Rangelow et.al. (2019).

The variability is distributed more or less evenly between β_R (aleatory) and β_U (epistemic). This is not necessarily the real distribution. Rather, the simultaneous sampling of aleatory (\rightarrow ground motion time histories) and epistemic (\rightarrow stiffness and damping parameters of soil and structures) **input** variability does not permit a distinction of the respective contribution to the total variability of the structural response factor F_{RS} . In the fragility analysis it has been **assumed** that $\beta_{R,RS}$ and $\beta_{U,RS}$ are equal. Again, it is referred to Rangelow et.al. (2019), where the relative contribution of β_R (aleatory) and β_U (epistemic) has been analyzed.

In this context it is also referred to the deterministic analysis results presented in Schmidl et.al. (2022), showing high variability of the seismic-induced stresses **within one deterministic soil class**. This variability cannot be explained by reasons other than i.) the variability of the ground motion intensity measures other than spectral acceleration and ii.) the **aleatory** variability of the ground motion time histories. It is recalled that – both in Schmidl et.al. (2022) and in the present paper - the use of recorded

ground motions as seed motions introduces variability in the intensity measures other than spectral acceleration (e.g. cumulative absolute velocity, Arias intensity, strong motion duration etc.).

RPVI - fuel assemblies

The main observation with respect to fuel assembly is that this failure mode has the **lowest variability** of all failure modes. This result has to do with the fact that failure is defined in terms of permanent inelastic deformation of the spacer grids. More specifically, the fragility is based on **two specific** time histories out of the 30 sets of time histories, namely the one leading to the **highest** impact force (“max”) and the one leading to the **median** of the sample of 30 impact forces. An incremental scaling of the corresponding two sets of excitation time histories of the core model is then performed, until the maximum permissible inelastic spacer grid deformation is reached. This approach is referred to as IDA (incremental dynamic analysis) in the earthquake engineering literature. The two resulting scaling factors are interpreted as the median and the 1,7% fractile.

It turns out that the variability **of the scaling factors** is significantly **smaller** than the variability of the impact forces. This phenomenon has been specifically studied in an earlier paper, Pellissetti (2017).

RPVI - core barrel upper flange

The core barrel flange is not governing the RPVI fragility in terms of the **HCLPF**, even though it is the most highly stressed part of the RPVI in the deterministic analysis, see Schmidl et.al. (2022), and as far as the **median** capacity is concerned. This related to the fact that the **variability** of the maximum CRDM stresses (→ failure mode “CRDM strength”) is significantly higher, see Figure 5.

RPVI – CRDM strength

This failure mode is **governing** the RPVI fragility – and hence the fragility of the reactor trip - in terms of the **HCLPF**. As mentioned above, this is related to the relatively high variability.

Again, this is in agreement with the deterministic analysis results in Schmidl et.al. (2022), showing that even within the same deterministic soil class the maximum stresses in the upper part of the CRDM exhibit significant variability among the seven deterministic time histories.

It is worth noting that **inelastic energy absorption** has not been credited for this failure mode. The reason being that significant inelastic deformations would not be compatible with the definition of the failure criterion of the failure mode “CRDM deformation”, which is based on a deformation level in the elastic range.

RPVI – CRDM deformation

This failure mode has the **highest variability** of all the considered failure modes. The HCLPF is not governing, though, since the median capacity is significantly higher than for the failure mode “CRDM strength”.

The large variability is related to the definition of the permissible deformation level of the CRDM, which is based on drop tests performed in the KOPRA experimental test facility, see Herr et.al. (2009). For each deformation level, a single drop test was conducted. No effect on the drop time was observed at any level of imposed deformation, including the maximum level. According to Porter et.al. (2007), Table 4, the tested level can be viewed as the 5% fractile of the capacity and composite variability parameter $\beta_c=0.4$ can be adopted. This **additional variability of the capacity factor** results in the higher variability of this failure mode.

Combined RPVI fragility

The following Figure 6 shows the fragility curves of the individual RPVI failure modes. In addition, a combined fragility curve is shown, defined as follows:

$$F_{RPVI,comb}(a) = P[I_{RPVI,any}|a], \quad I_{RPVI,any} = I_{RPVI,FA} \vee I_{RPVI,CB} \vee I_{RPVI,CRDM} \quad (6)$$

where $I_{RPVI,i}$ denotes the event “RPVI fails due to violation of failure criterion associated with sub-component i”. The calculation is performed using the composite fragilities of the individual failure modes. Conservatively, the three individual failure events are assumed to be independent. The combined fragility can then be evaluated for a given level a of the PGA by the basic formula for the probability of the union of independent events.

Two distinct regions of the combined fragility can be identified: in the low probability region – up to around 5% - the combined fragility is dominated by the contribution of the CRDM fragility. In the high probability region the contribution of the fuel assembly failure is predominant.

As a consequence, the HCLPF value of the combined fragility is essentially identical to the HCLPF of the CRDM fragility.

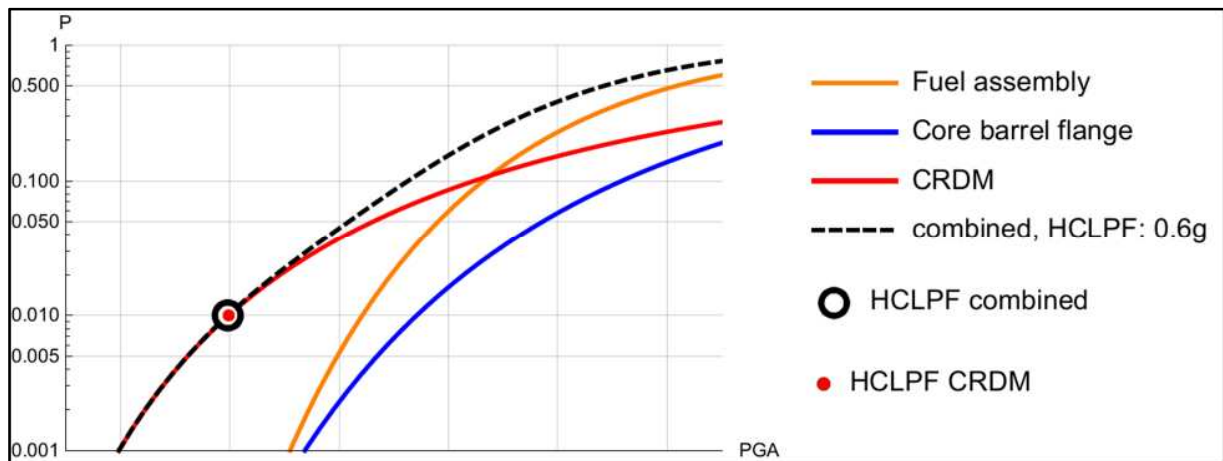


Figure 6. Fragility curves of individual RPVI internal failure modes and combined fragility curve (PGA intentionally not labeled)

CONCLUSIONS

The presented fragility analysis of NSSS components and piping, including main secondary piping in the reactor building, is based on 30 probabilistic time histories corresponding to the median UHS at $10^{-4}/\text{yr}$.

The supports of the main NSSS components have a very high seismic capacity. The loads from large breaks postulated in design ensure ample margins.

Large variability is associated with most failure modes, in particular the failure modes related to the CRDM. As a result, the HCLPF of the RPVI – and therefore the HCLPF of the reactor trip - is governed by the CRDM. For the FA the variability is substantially lower. This result confirms earlier studies showing

that in the non-linear evaluation of the relevant failure mode (permanent spacer grid deformation) a substantial amount of the uncertainties is absorbed.

NOMENCLATURE

CRDM Control rod drive mechanism
IDA Incremental dynamic analysis
LOCA Loss-of-coolant-accident
NSSS Nuclear steam supply system
RPVI Reactor pressure vessel internals
SSI Soil-structure interaction
UHS Uniform hazard spectra

REFERENCES

- ENSI (Eidgenoessisches Nuklearsicherheitsinspektorat, Swiss Federal Nuclear Safety Inspectorate). (2014) *Methodik deterministischer Nachweise der Schweizer Kernkraftwerke fuer Erdbeben der Stoerfallkategorien 2 und 3 (Methodology for deterministic demonstration of Swiss Nuclear Power Plants for Seismic Events in the Accident Categories 2 and 3)*, ENSI-AN-8567, Brugg, Switzerland (document language: German).
- EPRI. (2009). *Seismic Fragility Applications Guide Update*. Report 1019200. Palo Alto, CA.
- Fuetterer, E., Hilpert, R., Pellissetti, M., Nincic, V., Stäuble, S., Nykyforchyn, A. (2019). Coupled dynamic analysis of NSSS and reactor building including SSI for design-exceeding seismic ground motions, *Transactions, SMiRT-25*, Charlotte, NC, USA.
- Herr, E., Sykora, A., Kleideiter, A., Champonier, F. (2009). Qualification Test of the EPR Control Rod Drive Mechanism in the Full Scale Component Test Facility KOPRA, *Jahrestagung Kerntechnik (Annual Meeting on Nuclear Technology) 2009*, Dresden, Germany.
- Kennedy, R.P. and Ravindra, M.K. (1984). "Seismic fragilities for nuclear power plant risk studies". *Nuclear Engineering and Design*. 79, 47-68.
- Pellissetti, M., Keßler, H., Laudarin, F., Altieri, D., Nykyforchyn, A., Patelli, E., Klügel, J.-U. (2017). "Statistical analysis of impact forces and permanent deformations of fuel assembly spacer grids in the context of seismic fragility" *SMiRT-24*, Busan, Korea.
- Porter, K., Kennedy, R., Bachman, R. (2007). "Creating Fragility Functions for Performance-Based Earthquake Engineering." *Earthquake Spectra*, 23 (2) 471-489.
- Pellissetti, M., Kessler, H., Schmidl, J., Nykyforchyn, A., Staeuble-Akcaay, S. (2021). "Seismic performance of fuel assemblies and impact force correlations with intensity-compatible sets of recorded ground motion time histories," *Nuclear Engineering and Design*, 375: 111052.
- Rangelow, P., Richter, T., Nincic, V., Nykyforchyn, A., Stäuble, S., Pellissetti, M. (2019). Probabilistic SSI analysis of a reactor building to facilitate fragility assessment, *Transactions, SMiRT-25*, Charlotte, NC, USA.
- Schmidl, J., Pellissetti, M., Fuetterer, E., Hilpert, R., Nykyforchyn, A., Staeuble-Akcaay, S. (2022). "Deterministic and Probabilistic Evaluation of Seismic Loads on Reactor Pressure Vessel Internals Including Nonlinear Effects," *J. Pressure Vessel Technol*, 144(3): 031902.
- NAGRA (Nationale Genossenschaft für die Lagerung radioaktiver Abfälle) (2004). *Probabilistic Seismic Hazard Analysis for Swiss Nuclear Power Plant Sites (PEGASOS Project) – Final Report Volume 1 Text*, Wettingen, Switzerland.
- Stäuble-Akcaay, S., Nykyforchyn, A., Klügel, J.U. (2018). Seismic safety reassessment of NPP Gösgen after completion of site-specific probabilistic seismic hazard analysis. 16th ECEE, Greece.
- Swissnuclear (2014). *PEGASOS Refinement Project - Probabilistic Seismic Hazard Analysis for Swiss Nuclear Power Plant Sites – Volume 1 Summary Report*, Olten, Switzerland.